

# ac susceptibility and grain-boundary pinning strengths in $\text{YBa}_2\text{Cu}_3\text{O}_{7-\delta}$ and $\text{YBa}_2\text{Cu}_{2.985}\text{Ag}_{0.015}\text{O}_{7-\delta}$

S. L. Shindé, J. Morrill, D. Goland, D. A. Chance, and T. McGuire  
*IBM Thomas J. Watson Research Center, Yorktown Heights, New York 10598*

(Received 15 November 1989)

Estimation of the relative flux-pinning strengths of the matrix and the grain boundaries in polycrystalline oxide superconductors contributes to the understanding of their superconducting properties. Such understanding is further enhanced if measurements can be compared with those from materials with lattice substitution and doped grain boundaries. The ac susceptibilities of polycrystalline  $\text{YBa}_2\text{Cu}_3\text{O}_{7-\delta}$  and  $\text{YBa}_2\text{Cu}_{2.985}\text{Ag}_{0.015}\text{O}_{7-\delta}$  were measured as functions of temperature, ac-magnetic-field strength, and frequency. The presence of two loss peaks in the imaginary part of the susceptibility,  $\chi''$ , was confirmed by comparison of ac and dc measurements obtained on materials with different microstructures. One peak in  $\chi''$  was found to be associated with the matrix transition and the other, at lower temperatures, with weak-link behavior at grain boundaries. The model by K.-H. Müller for the field dependence of the peaks was used to estimate and compare the pinning-force densities in the matrix and at weak links for both pure and Ag-substituted  $\text{YBa}_2\text{Cu}_3\text{O}_{7-\delta}$ . In the temperature range (75–90 K) and field range (1–10 Oe, rms) studied, similar pinning forces,  $6 \times 10^8 \text{ T A m}^{-2}$ , for the matrix of the two materials were found, but the pinning-force densities at the weak links were higher for the Ag-substituted material by a factor of 1.5, i.e.,  $10^4 \text{ T A m}^{-2}$  for  $\text{YBa}_2\text{Cu}_{2.985}\text{Ag}_{0.015}\text{O}_{7-\delta}$  as compared to  $6 \times 10^3 \text{ T A m}^{-2}$  for  $\text{YBa}_2\text{Cu}_3\text{O}_{7-\delta}$ .

The measurement of ac susceptibility has provided important information on superconducting properties and ac losses in the polycrystalline high- $T_c$  superconductors.<sup>1–10</sup> In particular the loss component of the ac susceptibility has been used widely to probe the nature of weak links in polycrystalline superconductors.<sup>1,2,6,9</sup> We report here studies on ac and dc susceptibilities of the same samples to rationalize the ac losses in polycrystalline superconductors, and use a detailed study of the frequency and field dependence of the loss components to compare the flux pinning at grain boundaries in single-phase  $\text{YBa}_2\text{Cu}_3\text{O}_{7-\delta}$  and Ag-substituted  $\text{YBa}_2\text{Cu}_3\text{O}_{7-\delta}$ .

The real and imaginary parts of the complex ac susceptibility ( $\chi' + i\chi''$ ) represent two complementary aspects of flux dynamics in polycrystalline superconductors. The sharp drop in  $\chi'$  below the  $T_c$  has been related, in single crystals, to the temperature at which the flux penetrates to the center of the sample,<sup>11</sup> and in this sense the  $T_c$  derived from the ac  $\chi'$  really represents the “irreversibility temperature.”<sup>12,23</sup> In granular materials, the same argument can be extended for the matrix and the weak links to postulate two drops in  $\chi'$  at two temperatures.<sup>1</sup> The imaginary part,  $\chi''$ , represents the losses in the superconductor, and the peaks observed in  $\chi''$  can be interpreted in terms of losses incurred due to flux motion in the matrix and/or along the weak links in the polycrystalline microstructure. The study of  $\chi''$  variation with field and frequency of measurement has been used to estimate extrinsic properties, viz., transport critical-current densities,<sup>3,4</sup> flux-pinning barrier heights<sup>1</sup> etc., of the type-II superconductors.

The data on the ac susceptibility of polycrystalline superconductors reported in the literature is fraught with

seemingly disparate behavior. One group of researchers has reported only a single peak<sup>3,4,7,8</sup> in  $\chi''$ , while others have reported two,<sup>1,2,6,9</sup> and have interpreted the two peaks in terms of losses occurring within the grains and at the weak links (grain boundaries, inhomogeneities, etc.). Additionally, there has been some confusion as to whether the second peak in  $\chi''$ , often referred to as the “coupling peak,” shows any frequency dependence.<sup>1,3,4</sup> The effect of ac-field amplitude on the  $\chi''$  peaks has also not been clearly sorted out.<sup>2,3,7</sup> While some of these results can be put in perspective through theoretical arguments, a careful experimental study of the ac susceptibility of well-characterized polycrystalline superconductors is needed to explain the inconsistencies.

We present results of ac-susceptibility studies on polycrystalline superconductors with very carefully controlled microstructures, and with well characterized magnetic properties. The experiments reported here were designed (i) to confirm the presence of two peaks in  $\chi''$  in dense polycrystalline  $\text{YBa}_2\text{Cu}_3\text{O}_{7-\delta}$ , (ii) to prove that the “coupling peak” resulted in fact from ac-field-induced dissipation at the weak links, and most importantly (iii) to compare the flux-pinning behavior of the grain boundaries (GB's) in  $\text{YBa}_2\text{Cu}_3\text{O}_{7-\delta}$  and  $\text{YBa}_2\text{Cu}_{2.985}\text{Ag}_{0.015}\text{O}_{7-\delta}$  specimens through the field dependence of their matrix and “coupling” peaks.

Both the pure and Ag-substituted  $\text{YBa}_2\text{Cu}_3\text{O}_{7-\delta}$  samples were synthesized via the nitrate route.<sup>14</sup> The required mole fractions of 99.999% pure  $\text{Y}_2\text{O}_3$ ,  $\text{BaCO}_3$ ,  $\text{CuO}$ , and  $\text{AgNO}_3$  were dissolved in nitric acid diluted with high-purity deionized water and then spray dried to produce fine homogeneous powders. These powders were triple calcined at 950° C (with regrinding between runs)

and then ball milled before compaction at a pressure of 100 MPa. The pellets were then sintered and oxygenated using the annealing treatment described elsewhere.<sup>14,15</sup> The resulting samples always had greater than 95% density as measured using Archimedes's principle as well as optical microscopy, and an average grain size between 5 and 20  $\mu\text{m}$ .

All our samples were characterized using wet-chemical-analysis, x-ray diffractometry, and transmission electron microscopy (TEM) (Ref. 14) with microchemical analysis to determine the cation concentrations and crystal structure; dc magnetometry ( $\chi$  versus  $T$ ,  $M$  versus  $H$ ), flux-creep measurements, and measurement of  $J_c$  by magnetic and transport methods<sup>15</sup> were used to determine their superconducting properties. X-ray diffraction and TEM revealed <1% second phase in both samples. The dc  $\chi$  measurements, taken at 6 Oe (rms value for ac field), revealed 100% magnetic shielding for  $T$  below  $T_c$  for both the pure  $\text{YBa}_2\text{Cu}_3\text{O}_{7-\delta}$  and  $\text{YBa}_2\text{Cu}_{2.985}\text{Ag}_{0.015}\text{O}_{7-\delta}$  samples.  $J_c$  values estimated using the Bean model ( $J_c$  denotes the  $40M/d$  where  $M$  denotes the remanent moment and  $d$  denotes the thickness of the specimen) were found to be  $5 \times 10^5$  A/cm<sup>2</sup> at 5 K, for both samples, and the transport critical current at 5 K was found to be  $1.2 \times 10^3$  A/cm<sup>2</sup> for pure  $\text{YBa}_2\text{Cu}_3\text{O}_{7-\delta}$  and  $4 \times 10^3$  A/cm<sup>2</sup> for  $\text{YBa}_2\text{Cu}_{2.985}\text{Ag}_{0.015}\text{O}_{7-\delta}$ . Three  $\text{YBa}_2\text{Cu}_3\text{O}_{7-\delta}$  and two  $\text{YBa}_2\text{Cu}_{2.985}\text{Ag}_{0.015}\text{O}_{7-\delta}$  samples were used in this study and their average behavior used for comparison.

Measurements of  $\chi'$  and  $\chi''$  were performed using a Lake Shore Model 7000 ac susceptometer capable of measuring the complex ac susceptibility at discrete temperature points from 4.2 to 330 K, at rms applied fields from 0.4 to 800 A/m (5 mOe to 10 Oe), and at applied-field frequencies from 5 to 1000 Hz. The susceptibility readings were calibrated using a  $\text{Gd}_3\text{Ga}_5\text{O}_{12}$  single crystal, in addition to the factory calibration done using chrome potassium alum. The precision of the  $\chi$  measurements estimated from these calibration runs was  $99 \pm 1\%$ , with similar reproducibility. The phase angles at each frequency were also adjusted to obtain the true  $\chi'$  and  $\chi''$  components. Rectangular specimens, 2.5 mm  $\times$  4 mm  $\times$  200  $\mu\text{m}$  of  $\text{YBa}_2\text{Cu}_3\text{O}_{7-\delta}$  and  $\text{YBa}_2\text{Cu}_{2.985}\text{Ag}_{0.015}\text{O}_{7-\delta}$  were oriented under an optical microscope while being mounted on the holder to ensure that their surfaces would be parallel to the applied field, so that the demagnetization correction would be negligible. The variation from run to run on the same sample was thus minimized to less than 2%. The error bars included in the figures were calculated based on data for system-temperature stability and reproducibility (where needed) and combined errors in  $\chi$  value estimates (system precision, sample-volume-determination errors, and data reproducibility). Figures without error bars have errors less than the symbol sizes used for data presentation.

Figure 1 shows the ac-susceptibility data taken at 0.1 K intervals, and zero-field-cooled (ZFC) dc-susceptibility data at 1 K intervals, from 80 to 95 K both at 6 Oe (rms value for ac measurements), on a  $\text{YBa}_2\text{Cu}_3\text{O}_{7-\delta}$  sample. As shown in the Fig. 1(a), the sample exhibits perfect di-

amagnetism at 83 K, signified by the  $\chi'$  value of close to  $-1$  [dimensionless and in Systeme International (SI) units]. As the temperature increases,  $\chi'$  increases slowly until  $T = 87$  K, begins to level off, and then increases sharply near  $T = 89$  K, completing the transition by  $T = 90$  K. Above 90 K the  $\chi'$  trace remains at zero. The dc SQUID  $\chi$ -versus- $T$  data show no such two-step susceptibility behavior; the perfectly diamagnetic low-temperature value increases to zero smoothly between 88 and 90 K with no indication of a lower transition occurring in the material. This suggests that the initial increase of the  $\chi'$  curve reflects only ac phenomena, and is not related to a lower- $T_c$  phase.  $\chi''$  shows two distinct peaks as a function of temperature [Fig. 1(b)], one broad and located at the same temperature as the initial increase in  $\chi'$  (83–87) K, and the other sharp and located at the same temperature as the higher, sharper increase in  $\chi'$  (between 89 and 90 K).

Figure 2 shows a comparison of mass susceptibility  $\chi''$  (in SI units,  $\text{m}^3/\text{kg}$ ) versus  $T$  in a microcrack-free bulk  $\text{YBa}_2\text{Cu}_3\text{O}_{7-\delta}$  sample, before and after it was powdered to an average particle size less than its grain size as confirmed by optical microscopy. Figure 2 also shows  $\chi''$  versus  $T$  data for a large-grained ( $50 \times 300 \mu\text{m}^2$ ), 95%-dense sample with extensive microcracking resulting from anisotropic thermal contraction<sup>16</sup> of  $\text{YBa}_2\text{Cu}_3\text{O}_{7-\delta}$

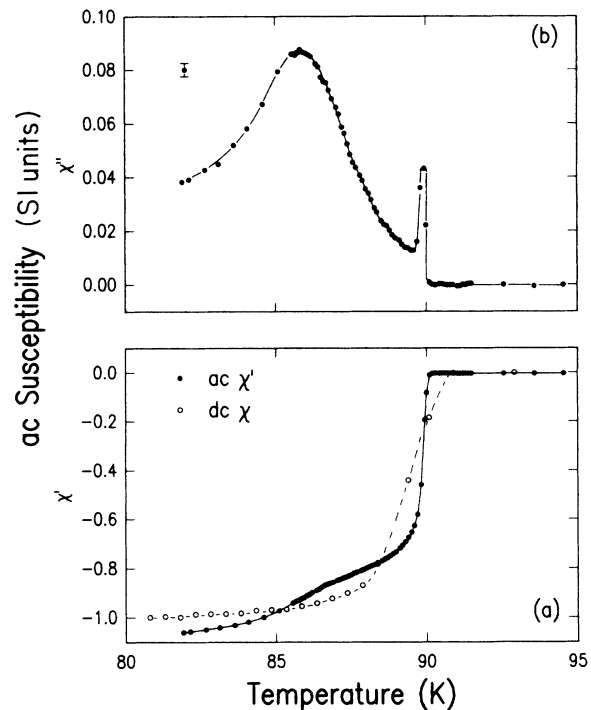


FIG. 1. Comparison of ac and dc susceptibilities for the same  $\text{YBa}_2\text{Cu}_3\text{O}_{7-\delta}$  sample. (a)  $\chi'$  for ac susceptibility (●) and ZFC branch of dc susceptibility (○). (b)  $\chi''$  showing the two peaks associated with losses in bulk and in weak links. All measurements were made at 6 Oe (rms for ac).

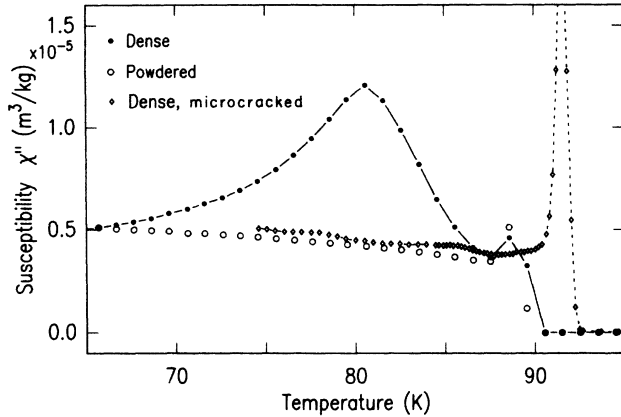


FIG. 2. Comparison of the imaginary part of ac susceptibility,  $\chi''$ , for bulk sample (●), and after it was powdered (○). Data for a 94% dense microcracked sample (◊) is also shown.

during cooling after oxygenation. Here only the microcrack-free dense sample shows two distinct peaks in  $\chi''$ . The absence of the second peak in  $\chi''$  for the powdered sample indicates that the ac losses registered in the second peak depend on intergrain coupling and hence occur most likely at the grain boundaries in polycrystalline type-II superconductors. The absence of this “coupling peak” in microcracked dense samples, in the powdered samples, and in the porous samples (that we have observed) (Ref. 17) can be used to explain the discrepancy between our two-component  $\chi''$  results and the one-component results found in the literature. The results indicate that a sample which is dense enough, and has sufficient grain coupling, will show two peaks in the  $\chi'$ -versus-temperature curve, while a more porous sample, tending to have a smaller amount of grain-boundary area per unit volume, will not register any appreciable grain-boundary ac losses. The groups reporting only one peak in the  $\chi''$  versus temperature curve, then, could have been working with samples with lower density and/or extensive microcracking that never achieve enough grain coupling to observe the peak associated

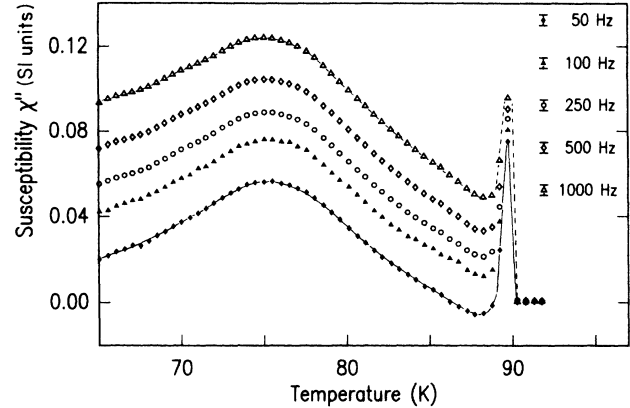


FIG. 3. Frequency dependence of  $\chi''$  for  $\text{YBa}_2\text{Cu}_3\text{O}_{7-\delta}$  at 6 Oe. The lowest frequency was 50 Hz (◆), and the highest 1000 Hz (△).

with grain-boundary losses; their  $\chi''$  measurements therefore are likely to be indicative of only the losses incurred within the grains themselves.

The results of our measurement of the frequency and field dependence of the “coupling peak” in  $\chi''$  for pure  $\text{YBa}_2\text{Cu}_3\text{O}_{7-\delta}$  and  $\text{YBa}_2\text{Cu}_{2.985}\text{Ag}_{0.015}\text{O}_{7-\delta}$  are represented in Figs. 3 and 4. Figure 3 presents  $\chi''$  versus temperature curves for pure  $\text{YBa}_2\text{Cu}_3\text{O}_{7-\delta}$  at  $H = 6$  Oe (rms) and  $f = 50, 100, 250, 500$ , and 1000 Hz, showing that the first peak, at 90 K, associated with the matrix transition is narrow ( $< 1$  K), and it does not show any frequency dependence. More importantly, Fig. 3 shows that the position of the coupling peak in  $\chi''$  does not appear to have any frequency dependence either. This result was obtained for all the fields for the  $\text{YBa}_2\text{Cu}_3\text{O}_{7-\delta}$  and  $\text{YBa}_2\text{Cu}_{2.985}\text{Ag}_{0.015}\text{O}_{7-\delta}$  samples, and was confirmed by parabolic fits to the peaks using data points near the apices. Nikolo and Goldfarb,<sup>1</sup> using Anderson's model for flux creep,<sup>18</sup> suggest that the temperature of the peak should be related to the frequency by the equation  $f = Ce^{(-E_a/kT_p)}$ , where  $C$  is a characteristic thermal-fluxon-hopping frequency and  $E_a$  is an approximate

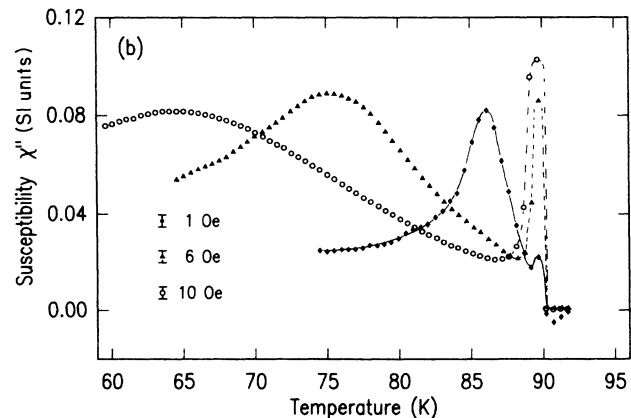
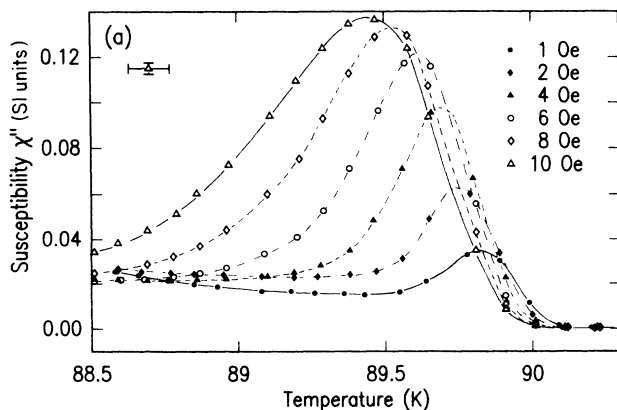


FIG. 4. (a) Field dependence of the matrix peak for a  $\text{YBa}_2\text{Cu}_3\text{O}_{7-\delta}$  sample. All samples tested showed a peak shift of  $0.5 \pm 0.1$  K. (b) Field dependence for the coupling peak of the same sample. A shift of about 23.5 K is observed for ac field of 10 Oe (rms).

(field-strength-dependent) value for the activation energy for flux creep at the grain boundaries, a measure of the grain-boundary pinning strength. From this equation, the temperature shift with frequency of the peak position can be derived as

$$d(1/T_{\text{peak}})/d \ln f = -k/E_a.$$

Nikolo and Goldfarb found an activation energy of about 6–8 eV at 1 Oe, derived from an observed peak shift of about 0.5 K over a frequency range from 10 to 1000 Hz. Our finding of no frequency dependence for all of our samples suggests that flux-creep activation energies at the grain boundaries of these samples were sufficiently high (higher than 25 eV at 6 Oe) that the temperature shift of the coupling peak was not detectable ( $<0.1$  K) within the frequency range explored in our experiment; Nikolo and Goldfarb, using the same frequency range, seem to have worked with samples showing lower activation energies. This seems plausible considering the high transport critical-current densities measured for our samples (4000 A/cm<sup>2</sup> at 5 K) and suggests that the method used by Nikolo and Goldfarb to relate the frequency dependence of the peak position to the grain-boundary pinning strength could be observable in our samples in the realm of frequencies much greater than 1000 Hz.

For both samples, however, the positions of the matrix and coupling peaks in  $\chi''$  did show dependence on the rms magnitude of the applied ac field, Figs. 4(a) and 4(b), and it is this dependence which we used to compare the pinning in the two samples. The matrix peak shift for a YBa<sub>2</sub>Cu<sub>3</sub>O<sub>7- $\delta$</sub>  sample is shown in Fig. 4(a) for fields from 1 to 10 Oe (rms). All the specimens tested showed peak shifts of  $0.5 \pm 0.1$  K; no effect of Ag doping was apparent in the field range studied. The average of all the peak shifts is about half of that reported by Goldfarb *et al.*,<sup>2</sup> 1 K, for the same field range. Figure 4(b) shows the field dependence of the coupling peak for one YBa<sub>2</sub>Cu<sub>3</sub>O<sub>7- $\delta$</sub>  sample. For the pure YBa<sub>2</sub>Cu<sub>3</sub>O<sub>7- $\delta$</sub>  samples, the peak

position shifted downward by  $(0.27 \pm 0.006)T_c$  as the rms field strength was increased from 1 to 10 Oe, and the peak width increased. For the YBa<sub>2</sub>Cu<sub>2.985</sub>Ag<sub>0.015</sub>O<sub>7- $\delta$</sub>  samples, the peak widened and shifted downward in position by  $(0.19 \pm 0.006)T_c$  for the same increase in field strength. The temperature shifts were normalized using  $T_c$  (position of matrix peak at 1 Oe) for individual specimens. In both cases, as before, peak positions were tracked using parabolic fits to points near the apices.

Malozemoff *et al.*,<sup>13</sup> studying single crystals of YBa<sub>2</sub>Cu<sub>3</sub>O<sub>7- $\delta$</sub> , have argued that the peak in  $\chi''$ , marking the onset of magnetic reversibility due to giant flux creep, should follow the “quasi-Almeida-Thouless line” or “irreversibility line” described originally by Müller *et al.*<sup>19</sup> for polycrystalline samples, which has been shown to follow the relation  $1 - T_{\text{peak}}/T_c = aH^q$ , where  $q$  has been found to be between  $\frac{2}{3}$  and  $\frac{3}{4}$ . As shown in Fig. 5(a), a plot of the peak-position variation with field for our samples superimposed on a plot of the irreversibility-line power law with  $q = \frac{2}{3}$  and  $\frac{3}{4}$ , our data do not show the predicted behavior; the lack of agreement with a unique power law was confirmed by a log-log plot of  $1 - T_{\text{peak}}/T_c$  versus  $H$ , which did not show a straight line and hence yielded no unique value for  $a$  or  $q$ . This is not surprising, however, when the polycrystalline nature of our samples is considered. The random distribution of grain orientations in the samples will naturally lead to a distribution of grain-boundary structures with different pinning behaviors and result in different irreversibility behaviors which cannot be expressed as a single unique power law. The disagreement of our data with the expected power-law behavior thus only highlights the fact that values for the grain-boundary pinning strengths of polycrystalline superconductors should be thought of as average, not as absolute values, as they describe a distribution of grain-boundary structures. Also, a comparison with ac susceptibility data taken with large dc fields<sup>13</sup> is inappropriate due to differences in the critical states within the single crystal and granular polycrystalline

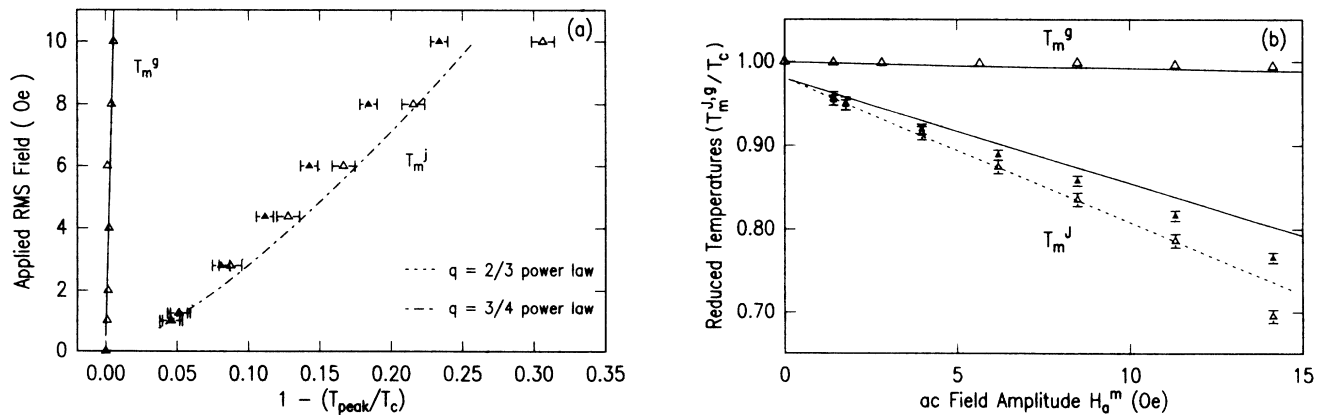


FIG. 5. (a) Field dependence of the matrix ( $T_m^g$ ) and coupling peak ( $T_m^j$ ) temperatures (normalized), for YBa<sub>2</sub>Cu<sub>3</sub>O<sub>7- $\delta$</sub>  ( $\Delta$ ) and for YBa<sub>2</sub>Cu<sub>2.985</sub>Ag<sub>0.015</sub>O<sub>7- $\delta$</sub>  ( $\blacktriangle$ ). Dotted and dot-dashed lines represent  $\frac{2}{3}$  and  $\frac{3}{4}$  power law behavior, respectively. (b) Comparison of the same data with Müller's model. The line for  $T_m^g$  vs  $H_a^m$  represents pinning force density of  $3 \times 10^8$  T A m<sup>-2</sup>, and the solid and dashed lines for  $T_m^j$  vs  $H_a^m$  represent  $1.21 \times 10^4$  and  $6.05 \times 10^3$  T A m<sup>-2</sup>, respectively.

samples.<sup>20,21</sup>

A recent paper by Müller<sup>21</sup> addresses the problem of quantifying the effect of applied field on the position of both the matrix peak  $T_m^g$  and the coupling peak  $T_m^j$  in  $\chi''$ , measured for polycrystalline materials. Müller accounts for the contributions from the intergranular and the intragranular components by setting up equations for the critical state in each component. He then estimates the field dependence of  $T_m^g$  and  $T_m^j$  to be proportional to the applied ac field amplitude  $H_a^m$  and inversely proportional to the pinning-force densities within the grains  $[\alpha_g(0)]$ , and at the weak links  $[\alpha_j(0)]$ . A comparison of our experimental data and the  $T_m^g$  and  $T_m^j$  versus  $H_a^m$  curves calculated by Müller for two different pinning force densities is shown in Fig. 5(b). The curves for  $T_m^j$  have been shifted by 1.9% (without other changes) to fit the data for  $\text{YBa}_2\text{Cu}_3\text{O}_{7-\delta}$ . The fit with the curve for  $\alpha_j(0) = 6.05 \times 10^3 \text{ T A m}^{-2}$  is quite good. The data for  $\text{YBa}_2\text{Cu}_{2.985}\text{Ag}_{0.015}\text{O}_{7-\delta}$  show a different slope and lie closer to the curve for  $\alpha_j(0) = 1.21 \times 10^3 \text{ T A m}^{-2}$  indicating higher pinning-force densities at the weak links in Ag-doped samples we studied. The matrix peak temperature  $T_m^g$  shifted by  $0.5 \pm 0.1 \text{ K}$  for the field amplitude of 14.14 Oe (10 Oe rms) for both  $\text{YBa}_2\text{Cu}_3\text{O}_{7-\delta}$  and  $\text{YBa}_2\text{Cu}_{2.985}\text{Ag}_{0.015}\text{O}_{7-\delta}$  samples (with the Ag-doped sample showing perhaps a somewhat smaller shift, 0.4 to 0.5 K). We compare this value to the 1 K shift for the curve calculated for  $\alpha_g(0) = 3 \times 10^8 \text{ T A m}^{-2}$  that is also observed in the data by Goldfarb *et al.*<sup>2</sup>

Müller's model seems to describe the data better than the equation for the "irreversibility line" developed for ac  $\chi$  measurements in large dc fields. The model uses average pinning-force densities to calculate the ac losses, and in this sense compares average behavior of the microstructure, which may make it more relevant for comparison of different microstructures. A comparison of the slopes of the two experimental data curves of  $T_m^j$  versus  $H_a^m$  then shows that the  $\text{YBa}_2\text{Cu}_{2.985}\text{Ag}_{0.015}\text{O}_{7-\delta}$  data slope is about 1.5 times less than that for the  $\text{YBa}_2\text{Cu}_3\text{O}_{7-\delta}$  data. This suggests that the average pinning strength at the grain boundaries is greater for

$\text{YBa}_2\text{Cu}_{2.985}\text{Ag}_{0.015}\text{O}_{7-\delta}$  than for  $\text{YBa}_2\text{Cu}_3\text{O}_{7-\delta}$  by a factor of about 1.5 in the temperature range of 65–90 K. Again it is important to remember that this value expresses an average, not an absolute relationship due to the wide distributions of grain orientations present in the polycrystalline samples.

In conclusion, we have confirmed that our samples of polycrystalline  $\text{YBa}_2\text{Cu}_3\text{O}_{7-\delta}$ , and  $\text{YBa}_2\text{Cu}_{2.985}\text{Ag}_{0.015}\text{O}_{7-\delta}$  exhibit two componenty in plots of both  $\chi'$  and  $\chi''$  versus temperature, and that the lower-temperature component can be attributed to ac phenomena and depends on grain coupling, a result which supports the idea that the peak at lower temperature in the  $\chi''$  versus temperature curve arises from ac losses incurred at the grain boundaries. We have also proposed that the observation of the expected two-componenty depends on the high density and resultant grain coupling of the samples being observed, which implies that the discrepancy between our two-component data and one-component data by others, is explainable in terms of differences in sample quality. We found no frequency dependence of the position of the coupling peak in the  $\chi''$  versus temperature curve for frequencies below 1000 Hz, indicating pinning strengths in excess of 25 eV at 75 K according to the model by Nikolo and Goldfarb.<sup>1</sup> We have used the dependence of the peak position on the rms-applied-field strength to compare the grain-boundary pinning in samples of  $\text{YBa}_2\text{Cu}_3\text{O}_{7-\delta}$  and  $\text{YBa}_2\text{Cu}_{2.985}\text{Ag}_{0.015}\text{O}_{7-\delta}$ . Using a simple approximate application of Müller's ac  $\chi$  model, we have argued that the average grain-boundary pinning strength of  $\text{YBa}_2\text{Cu}_{2.985}\text{Ag}_{0.015}\text{O}_{7-\delta}$  exceeds that of pure  $\text{YBa}_2\text{Cu}_3\text{O}_{7-\delta}$  by a factor of about 1.50 in the temperature range from 65 to 90 K.

#### ACKNOWLEDGMENTS

We would like to thank T. K. Worthington, Alex Malozemoff, and Y. Yeshurun for their critical comments on the manuscript and discussions during the course of this investigation, and T. Shaw for providing one of the  $\text{YBa}_2\text{Cu}_3\text{O}_{7-\delta}$  samples.

- <sup>1</sup>M. Nikolo and R. B. Goldfarb, *Phys. Rev. B* **39**, 6615 (1988).
- <sup>2</sup>R. B. Goldfarb, A. F. Clark, A. I. Braginski, and A. J. Panson, *Cryogenics* **27**, 475 (1987).
- <sup>3</sup>S. D. Murphy, K. Renouard, R. Crittenden, and S. M. Bhagat, *Solid State Commun.* **69**, 367 (1989).
- <sup>4</sup>F. Gomory and P. Lobotka, *Solid State Commun.* **66**, 645 (1988).
- <sup>5</sup>T. Ishida and H. Mazaki, *J. Appl. Phys.* **52**, 6798 (1981).
- <sup>6</sup>K. V. Rao, D.-X. Chen, J. Nogues, C. Politis, C. Gallo, and J. A. Gerber, *Proceedings of Symposium S*, edited by D. U. Gubser and M. Schluter (Materials Research Society, Pittsburgh, 1988), pp. 133–35.
- <sup>7</sup>Yu Mei and H. L. Luo, *J. Appl. Phys.* **64**, 2533 (1988).
- <sup>8</sup>Yasukage Oda, I. Nakada, T. Kohara, and K. Asayama, *Jpn. J. Appl. Phys.* **26**, L608 (1987).
- <sup>9</sup>A. F. Khoder, M. Couach, and B. Barbara, *Physica C* **153-155**, 1477 (1988).
- <sup>10</sup>M. Daeumling, J. Seutjens, and D. C. Larbalestier, *Physica C* **153-155**, 318 (1988).

- <sup>11</sup>T. K. Worthington, Y. Yeshurun, A. P. Malozemoff, R. M. Androfski, F. H. Holtzberg, and T. R. Dinger, *J. Phys. (Paris)* **49**, 2093 (1989).
- <sup>12</sup>Y. Yeshurun and A. P. Malozemoff, *Phys. Rev. Lett.* **60**, 2202 (1988).
- <sup>13</sup>A. P. Malozemoff, T. K. Worthington, Y. Yeshurun, and F. Holtzberg, *Phys. Rev. B* **38**, 7203 (1988).
- <sup>14</sup>S. L. Shinde, D. Goland, and D. Chance (unpublished).
- <sup>15</sup>S. L. Shinde, D. Goland, J. Yeshurun, T. McGuire, B. Bumble, and A. Kleinsasser (unpublished).
- <sup>16</sup>T. M. Shaw, S. L. Shinde, D. Dimos, R. F. Cook, P. R. Duncombe, and C. Kroll, *J. Mater. Res.* **4**, 248 (1989).
- <sup>17</sup>S. L. Shinde and J. Morrill (unpublished).
- <sup>18</sup>P. W. Anderson, *Phys. Rev. Lett.* **9**, 309 (1962).
- <sup>19</sup>K. A. Müller, M. Takashige, and J. G. Bednorz, *Phys. Rev. Lett.* **58**, 1143 (1987).
- <sup>20</sup>John R. Clem, H. R. Kerchner, and S. T. Sekula, *Phys. Rev. B* **14**, 1893 (1976).
- <sup>21</sup>K.-H. Müller, *Physica C* **159**, 717 (1989).